Chapter 1

Tau Decays into Hadrons

The τ lepton is an elementary particle with spin $1/2$ and a mass of $1.776\,86\,\mathrm{GeV}$ [**PDG2018**]. It is the only lepton heavy enough to decay into hadrons but also light enough for performing a low-energy QCD analysis. Its inclusive hadronic[1] decay ratio is given by

$$R_\tau = \frac{\Gamma(\tau \to \nu_\tau + \text{hadrons})}{\Gamma(\tau \to \nu_\tau e^- \overline{\nu}_e)} \tag{1.0.1}$$

and sensible to the strong coupling, due to its rather large value, at the m_τ^2 scale, of approximately 0.33. On the other hand $\alpha_s(m_\tau^2)$ is small enough to apply the OPE. The NP OPE contributions to the decay ratio are suppressed. The dimension two contributions of the OPE are proportional to the quark masses and have only a tiny contribution for light quarks. The dimension four contributions can be suppressed by applying weight functions, that do not have a monomial term x. E.g. the kinematic weight $\omega_\tau = (1-x)^2(1+2x) = 1 - 3x^2 + 2x^3$ is not sensitive to OPE corrections of dimension four. The dimension six contributions of the OPE are suppressed by a factor of $1/s^3$. They are further suppressed in the V+A channel, as the vector and axial-vector contributions have opposite signs and partly cancel themselves. Higher dimensional OPE contributions are suppressed by terms of $1/s^{2n}$ with $n \geqslant 4$. As a result, the perturbative contributions are dominant. They are known up to order $\mathcal{O}(\alpha_s^4)$ with a total contribution of 20% to R_τ [**Pich2016a**], which enables us to perform precise calculations of the inclusive τ decay ratio. Extracting α_s at low energies

[1] Meaning all decay channels with a hadron in its final state.

leads to low errors for α_s at high energies. The strong coupling and their errors run and get smaller with increasing energy. We compare the strong coupling at the Z-boson scale of around 91 GeV. Consequently the strong coupling at m_Z^2 from inclusive tau decays has especially low errors.

Hadronic τ decays permit one of the most precise determinations of the strong coupling α_s. Building on the previously presented QCDSR we will now elaborate the needed theory to extract α_s from the process of hadronic τ decays.

1.1 The Inclusive τ Decay Ratio

The theoretical expression of the inclusive hadronic τ decay ratio (eq. 1.0.1) is given by

$$R_\tau(s) = 12\pi \int_0^{m_\tau} \frac{ds}{m_\tau^2} \left(1 - \frac{s}{m_\tau^2}\right) \left[\left(1 + 2\frac{s}{m_\tau^2}\right) \operatorname{Im} \Pi^{(1)}(s) + \operatorname{Im} \Pi^{(0)}(s)\right], \quad (1.1.1)$$

where we omitted the electroweak correction (S_{EW}) and *Cabibbo-Kobayashi-Maskawa* (CKM) matrix element squared ($|V_{ud}|^2$). For brevity the two factors will be implicitly included. Equation 1.1.1 was first derived in [**Tsai1971**], using current algebra, a more recent derivation making use of the *optical theorem* can be taken from [**Schwab2002**]. Notice that we used the standard Lorentz decomposition into transversal ($J = 1$) and longitudinal ($J = 0$) components of **??** to display the hadronic decay ratio (eq. 1.1.1).

Applying Cauchy's theorem, as seen in **??**, to the eq. 1.1.1 we can rewrite the line integral into a closed contour integral

$$R_\tau = 6\pi i \oint_{s=m_\tau} \frac{ds}{m_\tau^2} \left(1 - \frac{s}{m_\tau^2}\right) \left[\left(1 + 2\frac{s}{m_\tau^2}\right) \Pi^{(1)}(s) + \Pi^{(0)}(s)\right]. \quad (1.1.2)$$

It is convenient to work with a slightly different combination of transversal and longitudinal components $\Pi^{(1+0)}$, which has been defined in **??** and is free of kinematic singularities. As a result, we can further rewrite the hadronic τ decay ratio into

$$R_\tau = 6\pi i \oint_{|s|=m_\tau} \frac{ds}{m_\tau^2} \left(1 - \frac{s}{m_\tau^2}\right)^2 \left[\left(1 + 2\frac{s}{m_\tau^2}\right) \Pi^{(1+0)}(s) - \left(\frac{2s}{m_\tau^2}\right) \Pi^{(0)}(s)\right]. \quad (1.1.3)$$

In the case of τ decays we only have to consider vector and axial-vector contributions of decays into up, down and strange quarks.

With eq. 1.1.3 we have a suitable physical quantity that can be theoretically calculated as well as experimentally measured. By using the QCDSR we apply a closed contour integral of radius s_0. As a result, we successfully avoid low energies at which the application of PT would be questionable. For example, by choosing a radius with the size of the τ mass $m_\tau \approx 1.78\,MeV$ the strong coupling has a perturbatively safe value of $\alpha_s(m_\tau^2) \approx 0.33$ **[Pich2016]**. Obviously, we would benefit even more from a contour integral over a bigger circumference, but τ decays are kinematically limited by their mass. Nevertheless, there are promising e^+e^- annihilation data, which yield inclusive decay ratio values up to $2\,GeV$ **[Boito2018][Keshavarzi2018]**.

1.1.1 Renormalisation Group Invariance

We have seen in **??**, that the two-point function is not a physical quantity, due to the dispersion relation (**??**) containing an unphysical polynom. Luckily for the vector correlator, appearing in hadronic τ decays, the polynom is just a constant. Consequently, we can take the derivative with respect to the momentum s to derive a physical quantity from the two-point function:

$$D(s) \equiv -s\frac{d}{ds}\Pi(s). \tag{1.1.4}$$

$D(s)$ is called the *Adler function* and fulfils, as all physical quantities, the RGE (**??**). The Adler function commonly has separate definitions for the longitudinal plus transversal and the solely longitudinal contributions:

$$D^{(1+0)}(s) \equiv -s\frac{d}{ds}\Pi^{(1+0)}(s), \qquad D^{(0)}(s) \equiv \frac{s}{m_\tau^2}\frac{d}{ds}(s\Pi^{(0)}(s)). \tag{1.1.5}$$

The two-point functions in eq. 1.1.3 can now be replaced with the help of partial integration

$$\int_a^b u(x)V(x)\,dx = \big[U(x)V(x)\big]_a^b - \int_a^b U(x)v(x)\,dx. \tag{1.1.6}$$

We will perform two separate computations for the $(1+0)$ and (0) case. Start-

ing by the transversal plus longitudinal contribution we get:

$$\begin{aligned} R_\tau^{(1)} &= \frac{6\pi i}{m_\tau^2} \oint_{|s|=m_\tau^2} \underbrace{\left(1-\frac{s}{m_\tau^2}\right)^2 \left(1+2\frac{s}{m_\tau^2}\right)}_{=u(x)} \underbrace{\Pi^{(1+0)}(s)}_{=V(x)} \\ &= \frac{6\pi i}{m_\tau^2} \left\{ \left[-\frac{m_\tau^2}{2} \left(1-\frac{s}{m_\tau^2}\right)^3 \left(1+\frac{s}{m_\tau^2}\right) \Pi^{(1+0)}(s) \right]_{|s|=m_\tau^2} \right. \\ &\quad \left. + \oint_{|s|=m_\tau^2} \underbrace{-\frac{m_\tau^2}{2} \left(1-\frac{s}{m_\tau^2}\right)^3 \left(1+\frac{s}{m_\tau^2}\right)}_{=U(x)} \underbrace{\frac{d}{ds}\Pi^{(1+0)}(s)}_{=v(x)} \right\} \\ &= -3\pi i \oint_{|s|=m_\tau^2 s} \frac{ds}{s} \left(1-\frac{s}{m_\tau^2}\right)^3 \left(1+\frac{s}{m_\tau^2}\right) \frac{d}{ds} D^{(1+0)}(s), \end{aligned} \tag{1.1.7}$$

where we fixed the integration constant to $c = -\frac{m_\tau^2}{2}$ in the second line and left the antiderivatives contained in the squared brackets untouched. If we parametrise the integral appearing in the expression in the squared brackets we can see that it vanishes:

$$\left[-\frac{m_\tau^2}{2} \left(1-e^{-i\phi}\right)^3 \left(1+e^{-i\phi}\right) \Pi^{(L+T)}(m_\tau^2 e^{-i\phi}) \right]_0^{2\pi} = 0, \tag{1.1.8}$$

where $s \to m_\tau^2 e^{-i\phi}$ and $(1-e^{-i\cdot 0}) = (1-e^{-i\cdot 2\pi}) = 0$. Repeating the same calculation for the longitudinal part yields

$$\begin{aligned} R_\tau^{(0)} &= \oint_{|s|=m_\tau^2} ds \left(1-\frac{s}{m_\tau^2}\right)^2 \left(-\frac{2s}{m_\tau^2}\right) \Pi^{(0)}(s) \\ &= -4\pi i \oint \frac{ds}{s} \left(1-\frac{s}{m_\tau^2}\right)^3 D^{(0)}(s). \end{aligned} \tag{1.1.9}$$

Consequently combining the transversal with the longitudinal contribution results in

$$R_\tau = -\pi i \oint_{|s|=m_\tau^2} \frac{ds}{s} \left(1-\frac{s}{m_\tau^2}\right)^3 \left[3\left(1+\frac{s}{m_\tau^2} D^{(1+0)}(s) + 4D^{(0)}(s)\right)\right]. \tag{1.1.10}$$

It is convenient to define $x = s/m_\tau^2$ such that we can rewrite the inclusive ratio into

$$R_\tau = -\pi i \oint_{|s|=m_\tau^2} \frac{dx}{x} (1-x)^3 \left[3(1+x) D^{(1+0)}(m_\tau^2 x) + 4D^{(0)}(m_\tau^2 x)\right], \tag{1.1.11}$$

which will be the final expression used to express the inclusive τ decay ratio.

1.2 Theoretical Computation of R_τ

The previously derived expression for the τ decay ratio is at first approximation equal to the number of colours [**Peskin1995**]

$$R_\tau \approx N_c. \tag{1.2.1}$$

If we take the perturbative δ_{pt} and non-perturbative δ_{npt} contributions into account we can organise the vector and axial-vector inclusive decay ratio as

$$R^{\omega}_{\tau,V/A} = \frac{N_c}{2}\left(1 + \delta^{\omega}_{pt} + \delta^{\omega}_{npt}\right). \tag{1.2.2}$$

Note that the factor $1/2$ comes from the fact, that in the chiral limit the vector and axial-vector contributions are equal. The dependence on the chosen weight function ω is reflected in the upper indices.

For the kinematic weight (**??**), which appears naturally in the τ decay ratio, we have a dominant perturbative contribution of $\delta_{pt} \approx 20\%$ to R_τ [**Pich2013**] and a minor, but non-negligible, NP contribution of $\delta^{NP}_{V+A} \lesssim 1\%$ [**Jamin2013**] for the $V + A$-channel.

In the following, we want to derive the theoretical expressions needed to calculate both of the corrections to eq. 1.2.2 starting with the perturbative one.

1.2.1 The Perturbative Contribution

The perturbative contribution δ_{pt} to the inclusive τ decay ratio corresponds to the first term of the OPE. Currently, the perturbative expansion has been calculated to fourth order $\mathcal{O}(\alpha_s^4)$. Due to their role as dominant corrections, their uncertainties from unknown higher-order corrections dictate the final error of the determination of the strong coupling [**Pich2016**].

We will treat the correlator in the chiral limit, in which the scalar and pseudoscalar contributions of the two-point function vanish and the axial and vectorial contributions are equal. As a result, we can focus on the vector correlator $\Pi_V(s)$, which can be expanded as a sum over different orders of α

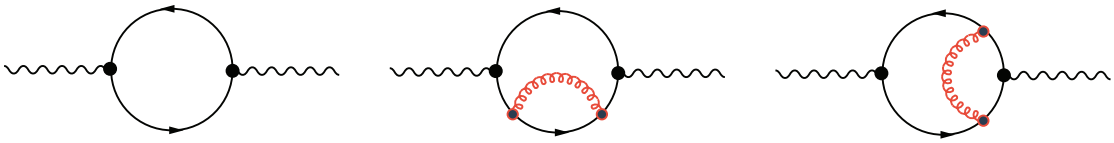

Figure 1.1: Feynman loop diagrams to calculate the $c_{n,k}$ coefficients of the expanded correlator $\Pi_V^{(1+0)}$. The internal red lines represent gluons. Diagram a) represents the parton model and diagrams b) and c) represent higher order corrections.

[Beneke2008]:

$$\Pi_V^{(1+0)}(s) = -\frac{N_c}{12\pi^2}\sum_{n=0}^{\infty} a_\mu^n \sum_{k=0}^{n+1} c_{n,k} L^k \quad \text{with} \quad L \equiv \ln\frac{-s}{\mu^2}, \tag{1.2.3}$$

where we defined $a_\mu \equiv \alpha(\mu)/\pi$. The coefficient $c_{n,k}$ up to two-loop order can be obtained by Feynman diagram calculations. With the diagrams of fig. 1.1 we can calculate the one-loop result of the correlator **[Jamin2006]**

$$\Pi^B(q^2)\Big|^{1-\text{loop}} = \frac{N_c}{12\pi^2}\left(\frac{1}{\hat{\epsilon}} - \log\frac{(-q^2 - i0)}{\mu^2} + \frac{5}{3} + \mathcal{O}(\epsilon)\right), \tag{1.2.4}$$

where $\Pi^B_{\mu\nu}(q^2)$ is the bare two-point function[2]. This result can then be used to extract the first two coefficients of the correlator expansion given in eq. 1.2.3

$$c_{0,0} = -\frac{5}{3} \qquad \text{and} \qquad c_{0,1} = 1. \tag{1.2.5}$$

The second loop can also be calculated by diagram techniques resulting in **[Boito2011]**

$$\Pi_V^{(1+0)}(s)\Big|^{2-\text{loop}} = -\frac{N_c}{12\pi^2} a_\mu \log(\frac{-s}{\mu^2}) + \cdots. \tag{1.2.6}$$

From the above equation we can then extract the Adler coefficient $c_{1,1} = 1$.

Beginning from three loop diagrams the algebra becomes exhausting and one has to use dedicated algorithms to compute the higher loops. The third loop calculations have been done in the late seventies **[Chetyrkin1979, Dine1979, Celmaster1979]**. The four loop evaluation has been completed a little more

[2]The term $1/\hat{\epsilon}$, which is of order zero in α_s, is not present in the Adler function or the imaginary part of the correlator.

than ten years later [**Gorishnii1990**, **Surguladze1990**]. The highest calculated loop, that amounts to α_s^4, was published in 2008 [**Baikov2008**] almost 20 years later.

By fixing the number of colours to $N_c = 3$, we can write the missing coefficients up to order four in α_s:

$$\begin{aligned} c_{2,1} &= \frac{365}{24} - 11\zeta_3 - \left(\frac{11}{12} - \frac{2}{3}\zeta_3\right) N_f \\ c_{3,1} &= \frac{87029}{288} - \frac{1103}{4}\zeta_3 + \frac{275}{6}\zeta_5 \\ &\quad - \left(\frac{7847}{216} - \frac{262}{9}\zeta_3 + \frac{25}{9}\zeta_5\right) N_f + \left(\frac{151}{162} - \frac{19}{27}\zeta_3\right) N_f^2 \\ c_{4,1} &= \frac{78631453}{20736} - \frac{1704247}{432}\zeta_3 + \frac{4185}{8}\zeta_3^2 + \frac{34165}{96}\zeta_5 - \frac{1995}{16}\zeta_7, \end{aligned} \tag{1.2.7}$$

where we used the flavour number $N_f = 3$ for the last line.

The six loop calculation has until today not been computed, but Beneke and Jamin [**Beneke2008**] made an educated guess to estimate the coefficient

$$c_{5,1} \approx 283 \pm 283. \tag{1.2.8}$$

We often see $c_{5,1}$ applied to estimate the perturbative errors related to missing higher order contributions.

In stating the coefficients $c_{n,k}$ of the correlator expansion we have restricted ourselves to k indices equal to one. This is due to the RGE, which relates coefficients with k different than one to coefficients with k equal to one ($c_{n,1}$). Consequently, the vector correlator $\Pi_V^{1+0}(s)$ needs to be transformed into a physical quantity, which can be achieved by applying the derivative with respect to s, yielding the previously defined Adler function (eq. 1.1.5). The correct expression for the correlator expansion in eq. 1.2.3 is then given by

$$D_V^{(1+0)} = -s\frac{d\Pi_V^{(1+0)}(s)}{ds} = \frac{N_c}{12\pi^2}\sum_{n=0}^{\infty} a_\mu^n \sum_{k=1}^{n+1} k c_{n,k} L^{k-1}, \tag{1.2.9}$$

where we used $dL^k/ds = k\ln(-s/\mu^2)^{k-1}(-1/\mu^2)$. Applying the RGE (**??**) to the scale-invariant Adler function yields

$$-\mu\frac{d}{d\mu}D_V^{(1+0)} = -\mu\frac{d}{d\mu}\left(\tfrac{\partial}{\partial L}\,dL + \tfrac{\partial}{\partial a_s}\,da_s\right)D_V^{(1+0)} = \left(2\tfrac{\partial}{\partial L} + \beta\tfrac{\partial}{\partial a_s}\right)D_V^{(1+0)} = 0, \tag{1.2.10}$$

where we made use of the β-function, which is defined in **??**, and of the expression $dL/d\mu = -2/\mu$.

The relation between the correlator expansion coefficients can then be taken by calculating the Adler function for a desired order and plugging it into the RGE. For example, the Adler function to the second order in α_s is expressed as

$$D(s) = \frac{N_c}{12\pi^2}\left[c_{01} + a_\mu(c_{11} + 2c_{12}L) + a_\mu^2(c_{21} + 2c_{22}L + 3c_{23}L^2)\right]. \tag{1.2.11}$$

Inserting the newly obtained Adler function into eq. 1.2.10 yields

$$4a_\mu c_{12} + 2a_\mu^2(2c_{22} + 6c_{23}L) + \beta_1 a_\mu^2(c_{11} + 2c_{12}L) + \mathcal{O}(a_\mu^3) = 0. \tag{1.2.12}$$

From this equation, we can compare the coefficients order by order in α_s to constrain the Adler function coefficients. At order α_μ only the c_{12} term is present and has to be zero. For $\mathcal{O}(a_\mu^2 L)$ solely c_{23} exists as $c_{12} = 0$ and has to vanish. Finally for $\mathcal{O}(a)$ we can relate c_{22} with c_{11} resulting in

$$c_{12} = 0, \quad c_{22} = \frac{\beta_1 c_{11}}{4} \quad \text{and} \quad c_{23} = 0. \tag{1.2.13}$$

Implementing the newly obtained Adler coefficients we can write out the Adler function to the first order:

$$D(s) = \frac{N_c}{12\pi^2}\left[c_{01} + c_{11}a_\mu\left(c_{21} - \frac{1}{2}\beta_1 c_{11}L\right)a_\mu^2\right] + \mathcal{O}(a_\mu^3). \tag{1.2.14}$$

We have used the RGE to relate Adler function coefficients and thus only need to know the coefficients of type $c_{n,1}$. Unfortunately, as we will see in the following section, the RGE gives us two different choices to compute the perturbative contribution to the inclusive τ decay ratio.

Renormalisation Group Summation

By making use of the RGE we have to decide about the order of mathematical operations we perform. As the all order perturbative contribution δ_{pt} is independent on the scale μ we are confronted with two choices, namely FOPT and CIPT. Each of them yields a different result, which is the main source of error in extracting the strong coupling from τ decays.

Working in the chiral limit additionally permits us to neglect the longitudinal contribution $D^{(0)}$, in eq. 1.1.11 of the perturbative contribution δ_{pt} of R_τ (eq. 1.2.2). Thus inserting the expansion of $D_V^{(1+0)}$ into the hadronic τ decay width eq. 1.1.11 yields

$$\delta_{pt} = \sum_{n=1}^{\infty} a_\mu^n \sum_{k=1}^{n} k c_{n,k} \frac{1}{2\pi i} \oint_{|x|=1} \frac{dx}{x} (1-x)^3 (1+x) \log\left(\frac{-m_\tau^2 x}{\mu^2}\right)^{k-1}, \tag{1.2.15}$$

where the contributions from the vector and axial-vector correlator are identical in the massless case.

To continue evaluating the perturbative part we can now either follow the description of FOPT or CIPT.

In FOPT, we fix the renormalisation scale at the τ mass ($\mu^2 = m_\tau^2$), which leaves us with the integration over the logarithm, as can be seen in

$$\delta_{FOPT}^{(0)} = \sum_{n=1}^{\infty} a(m_\tau^2)^n \sum_{k=1}^{n} k c_{n,k} J_{k-1}, \tag{1.2.16}$$

where the contour integrals J_l are defined by

$$J_l \equiv \frac{1}{2\pi i} \oint_{|x|=1} \frac{dx}{x} (1-x)^3 (1+x) \log^l(-x). \tag{1.2.17}$$

The integrals J_l up to order α_s^4 are given by [**Beneke2008**]:

$$J_0 = 1, \quad J_1 = -\frac{19}{12} \quad J_2 = \frac{265}{72} - \frac{1}{3}\pi^2, \quad J_3 = -\frac{3355}{288} + \frac{19}{12}\pi^2. \tag{1.2.18}$$

Using FOPT the strong coupling $a(\mu)$ is fixed at the τ mass scale $a(m_\tau^2)$ and can be taken out of the closed-contour integral. Thus we solely have to integrate over the logarithms $\log(x)$.

Using CIPT, on the contrary, we can sum the logarithms by setting the scale to $\mu^2 = -m_\tau^2 x$ in eq. 1.2.15, resulting in:

$$\delta_{CI}^{(0)} = \sum_{n=1}^{\infty} c_{n,1} J_n^a(m_\tau^2), \tag{1.2.19}$$

where the contour integrals J_n^a are defined by

$$J_n^a(m_\tau^2) \equiv \frac{1}{2\pi i} \oint_{|x|=1} \frac{dx}{x} (1-x)^3 (1+x) a^n(-m_\tau^2 x). \tag{1.2.20}$$

Note that all logarithms vanish, except the ones with index $k = 1$:

$$\log(1)^{k-1} = \begin{cases} 1 & \text{if } k = 1, \\ 0 & k \neq 1 \end{cases} \tag{1.2.21}$$

which selects the Adler function coefficients $c_{n,1}$. Handling the logarithms left us with the integration of the strong coupling $\alpha_s(-m_\tau^2 x)$ over the closed-contour $\oint_{|x|=1}$, which now depends on the integration variable x.

In general, we have to decide if we want to perform a contour integration with a constant strong coupling parameter and variable logarithms (FOPT) or "constant logarithms" and a running coupling (CIPT). To emphasise the differences in both approaches we can calculate the perturbative contribution $\delta^{(0)}$ to R_τ for the two different prescriptions yielding [**Beneke2008**]

$$\begin{aligned} & \alpha_s^2 \qquad \alpha_s^2 \qquad \alpha_s^3 \qquad \alpha_s^4 \qquad \alpha_s^5 \\ \delta^{(0)}_{\text{FOPT}} &= 0.1082 + 0.0609 + 0.0334 + 0.0174(+0.0088) = 0.2200(0.2288) \qquad (1.2.22) \\ \delta^{(0)}_{\text{CIPT}} &= 0.1479 + 0.0297 + 0.0122 + 0.0086(+0.0038) = 0.1984(0.2021). \qquad (1.2.23) \end{aligned}$$

The series indicate, that CIPT converges faster and that both series approach a different value. FOPT has larger contributions than CIPT, which leads to a smaller strong coupling if using FOPT. The discrepancy, between FOPT and CIPT, represents currently the biggest theoretical uncertainty for extracting the strong coupling.

As today FOPT or CIPT are equally valid approaches to calculate the perturbative contributions, even though it has been stated by Beneke et al. [**Beneke2008**] to favour the former. Within this work, we will further elaborate on the consistency of FOPT and do not state our results in CIPT.

1.2.2 The Non-Perturbative OPE Contributions

The perturbative contributions to the sum rule are the dominant one, but NP have to be taken into account. The contributions of the NP part can be quoted as [**Jamin2013**]

$$\delta^{\text{NP}}_{\text{V+A,FOPT}} = -0.086(80), \tag{1.2.24}$$

which are small, but not negligible. The NP OPE contributions are commonly categorised by even, increasing dimensions. Contributions of dimension larger than eight are normally neglected, due to the increasing suppression by factors of $1/s^D$, where D stands for the corresponding dimension.

The dimension two contributions are proportional to the quark masses and vanish while working in the chiral limit. Consequently, we will neglect them and start by stating the $D = 4$ contributions.

1.2.3 Dimension Four Corrections

The next apparent OPE contributions are of dimension four. Here we have to take the terms with masses to the fourth power (m^4) into account, the quark condensate multiplied by a mass ($m\langle\overline{q}\,q\rangle$) and the gluon condensate ($\langle GG\rangle$). The resulting expression can be taken from the appendix of [**Pich1999**], yielding:

$$D_{ij}^{(1+0)}(s)\Big|_{D=4} = \frac{1}{s^2}\sum_n \Omega^{(1+0)}(s/\mu^2)a^n, \tag{1.2.25}$$

where the $\Omega^{(1+0)}(s/\mu^2)$ is given by

$$\begin{aligned}\Omega_n^{(1+0)}(s/\mu^2) \;=\; & \frac{1}{6}\langle aGG\rangle p_n^{(1+0)}(s/\mu^2) + \sum_k m_k\langle\overline{q}_k q_k\rangle r_n^{(1+0)}(s/\mu^2)\\ & + 2\langle m_i\overline{q}_i q_i + m_j\overline{q}_j q_j\rangle q_n^{(1+0)}(s/\mu^2) \pm \frac{8}{3}\langle m_j\overline{q}_i q_i + m_i\overline{q}_j q_j\rangle t_n^{(1+0)}\\ & - \frac{3}{\pi^2}(m_i^4 + m_j^4)h_n^{(1+0)}(s/\mu^2) \mp \frac{5}{\pi^2}m_i m_j(m_i^2 + m_j^2)k_n^{(1+0)}(s/\mu^2)\\ & + \frac{3}{\pi^2}m_i^2 m_j^2 g_n^{(1+0)}(s/\mu^2) + \sum_k m_k^4 j_n^{(1+0)}(s/\mu^2) + 2\sum_{k\neq l} m_k^2 m_l^2 u_n^{(1+0)}(s/\mu^2).\end{aligned} \tag{1.2.26}$$

The perturbative expansion coefficients are known to second order $\mathcal{O}(a^2)$ for the condensate contributions,

$$\begin{array}{lll} p_0^{(1+0)} = 0, & p_1^{(1+0)} = 1, & p_2^{(1+0)} = \frac{7}{6},\\ r_0^{(1+0)} = 0, & r_1^{(1+0)} = 0, & r_2^{(1+0)} = -\frac{5}{3} + \frac{8}{3}\zeta_3 - \frac{2}{3}\log(s/\mu^2),\\ q_0^{(1+0)} = 1, & q_1^{(1+0)} = -1, & q_2^{(1+0)} = -\frac{131}{24} + \frac{9}{4}\log(s/\mu^2)\\ t_0^{(1+0)} = 0 & t_1^{(1+0)} = 1, & t_2^{(1+0)} = \frac{17}{2} + \frac{9}{2}\log(s/\mu^2). \end{array} \tag{1.2.27}$$

while the m^4 terms have been only computed to first order $\mathcal{O}(a)$

$$\begin{aligned}
h_0^{(1+0)} &= 1 - 1/2\log(s/\mu^2), & h_1^{(1+0)} &= \tfrac{25}{4} - 2\zeta_3 - \tfrac{25}{6}\log(s/\mu^2) - 2\log(s/\mu^2)^2,\\
k_0^{(1+0)} &= 0, & k_1^{(1+0)} &= 1 - \tfrac{2}{5}\log(s/\mu^2),\\
g_0^{(1+0)} &= 1, & g_1^{(1+0)} &= \tfrac{94}{9} - \tfrac{4}{3}\zeta_3 - 4\log(s/\mu^2),\\
j_0^{(1+0)} &= 0, & j_1^{(1+0)} &= 0,\\
u_0^{(1+0)} &= 0, & u_1^{(1+0)} &= 0.
\end{aligned} \tag{1.2.28}$$

The gluon and quark condensates depend on the scale μ^2, but we can express them in the form of the scale-invariant gluon- and quark-condensate [**Spiridonov1988**], which are combinations of the minimally subtracted operators

$$\begin{aligned}
\beta_1\langle aG^2\rangle_I \equiv \beta(s)\langle G^{\mu\nu}_{(a)}G^{(a)}_{\mu\nu}\rangle + 4\gamma(a)\sum_{i=u,d}\langle m_i\overline{q}_i q_i\rangle\\
-\frac{3}{4\pi^2}\sum_{i,j=u,d} m_i^2 m_j^2\gamma_0^{ij}(a)
\end{aligned} \tag{1.2.29}$$

$$\langle m_i\overline{q}_j q_j\rangle_I \equiv \langle m_i\overline{q}_j q_j\rangle + \frac{3m_i m_j^3}{7\pi^2 a}\left\{1 - \frac{53}{24}a + \mathcal{O}(a^2)\right\}, \tag{1.2.30}$$

where $\gamma_0^{ij}(a) = -2 - 8/3a$. During this work, we will insert the known invariant quark condensates (see **??**) as constants and state our results for the invariant gluon condensate.

1.2.4 Dimension Six and Eight Corrections

Our application of dimension six contributions is founded in [**Braaten1991**]. They have previously been calculated beyond leading order by [**Lanin1986**]. The operators appearing are the masses to the power six (m^6), the four-quark condensates ($\langle\overline{q}\,q\overline{q}\,q\rangle$), the three-gluon condensates ($\langle g^3G^3\rangle$) and lower dimensional condensates multiplied by the corresponding masses, such that in total the mass dimension of the operators will be six. The largest contributions come from the 4-quark operators. The three-gluon condensate does not contribute at leading order [**Hubschmid1982**] and is neglected. Operators proportional to the light quark masses will also be neglected. The resulting contributions of dimension six operators have been calculated in [**Lanin1986**] and lead to many

operators, which until today cannot be accurately determined by phenomenology methods. To reduce the number of operators we can make use of the *vacuum saturation approximation* (VSA) [**Beneke2008**, **Braaten1991**, **Shifman1978**]. The VSA is used to express the four-quark condensates as squares of quark-antiquark condensates ($\langle\overline{q}_i q_j\rangle^2$. If we apply the VSA to first order in α_s, we can write out the dimension six OPE contributions

$$D^{1+0}_{ij,V/A}(s)\Big|_{D=6} = \frac{32\pi^2}{3}a(\mu)\frac{\langle\overline{q}_i q_i(\mu)\rangle\langle\overline{q}_j q_j\rangle}{s^3} - \frac{32}{7}\pi^2 a_\mu \frac{\langle\overline{q}_i q_i\rangle^2\langle\overline{q}_j q_j\rangle^2}{s^3}. \quad (1.2.31)$$

Unfortunately, the scaling properties of the dimension six contributions are inconsistent with the scaling properties of the 4-quark operators [**Narison1983**, **Jamin1985**] and terms of order α_s^2 are usually ignored. In addition to the scaling problematic, the VSA is known to underestimate the dimension six contribution [**Launer1983**].

In our work we, take the simplest approach possible. We introduce an effective dimension six coefficient $\rho^{(6)}_{V/A}$ divided by the appropriate power in s

$$D^{(1+0)}_{ij,V/A}(s)\Big|_{D=6} = 3\frac{\rho^{(6)}_{V/A}}{s^3}. \quad (1.2.32)$$

Here we also neglected the scale dependence of the dimension six operators, which is determined by the anomalous dimension. We have calculated the leading-order anomalous dimension matrices corresponding to the dimension six four-quark operators of flavour non-diagonal, as well as flavour diagonal, mesonic vector and axial-vector currents in [**Boito2015**].

For higher dimensional contributions the situation is not better than the dimension six one. Up to dimension twelve we will keep the simplest approach of introducing a parameter for every OPE dimension leading to

$$D^{(1+0)}_{ij,V/A}\Big|_{D=8} = 4\frac{\rho^{(8)}_{V/A}}{s^4}, \quad D^{(1+0)}_{ij,V/A}\Big|_{D=10} = 5\frac{\rho^{(10)}_{V/A}}{s^5} \quad \text{and} \quad D^{(1+0)}_{ij,V/A}\Big|_{D=12} = 6\frac{\rho^{(12)}_{V/A}}{s^6}. \quad (1.2.33)$$

The NP contribution of dimension twelve is the highest order that we are going to implement. Higher orders will be neglected. Next, to the NP treatment of the OPE, we have to discuss possible DV.

1.3 Duality Violations

As seen in **??** we have to assume quark-hadron duality for the QCDSR to work. Unfortunately, duality is always to some extent broken through so-called DV, which are well known [**Cata2008**, **Cata2009**]. Experimental data show an oscillating behaviour that cannot be reproduced by the OPE. Moreover, in the large N_c limit, it can be shown that DV have an exponential decreasing, sinusoidal appearance [**Cata2005**]. Consequently, for the cases with apparent DV, we have to include the corrections coming from DV and adapt eq. 1.2.2, leading to

$$R^{\omega}_{\tau,V/A} = \frac{N_c}{2} S_{EW} |V_{ud}|^2 \left(1 + \delta^{\omega}_{pt} + \delta^{\omega}_{npt} + \delta^{\omega}_{dv}\right), \tag{1.3.1}$$

where we extracted δ_{dv} from δ_{npt}, even though DV are NP. The DV corrections have been modelled with the following ansatz [**Cata2009**]

$$\rho^{DV}_{V/A}(s) = e^{-(\delta_{V/A} + \gamma_{V/A} s)} \sin(\alpha_{V/A} + \beta_{V/A} s), \tag{1.3.2}$$

which contains four parameters for the vector and another four parameters for the axial-vector contribution. Note that for fitting the kinematic weight in the V-channel, which is known to be sensible for DV at lower energies [**Boito2011a**], we would have seven parameters instead of only three. By including the model, we append the DV as an additional term in the inclusive τ decay ratio

$$R_{\tau,V/A} = -\pi i \oint_{|s|=m_\tau^2} \frac{dx}{x}(1-x)^3 \left[3(1+x)D^{(1+0)}(m_\tau^2 x) + 4D^{(0)}(m_\tau^2 x)\right] + \mathcal{D}_{V/A}(m_\tau^2), \tag{1.3.3}$$

where the DV contributions would be given as

$$\mathcal{D}_{\omega}(m_\tau^2) = -12\pi^2 \int_{m_\tau^2}^{\infty} \frac{ds}{m_\tau^2} \omega(s) \rho_{V/A}. \tag{1.3.4}$$

1.3.1 Pinched Weights to avoid DVs

The general QCDSR (**??**) contain a weight function ω, which is not only used to suppress higher order dimensions, but also DV. The weights that suppress DV are so-called pinched weights of the form

$$\omega(s) = \left(1 - \frac{s}{m_\tau^2}\right)^k, \tag{1.3.5}$$

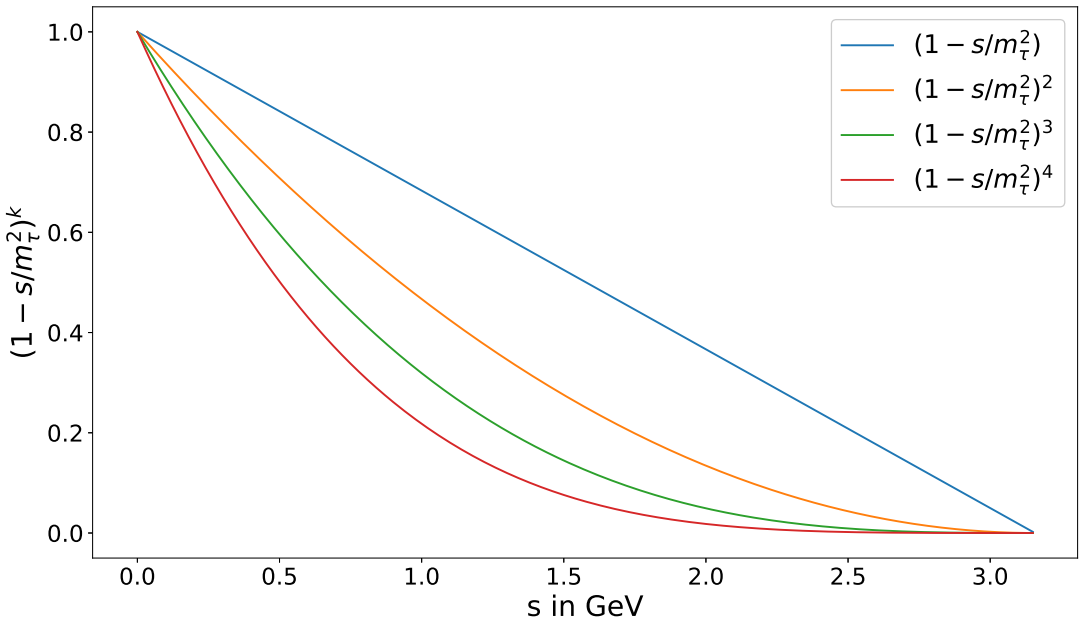

Figure 1.2: Pinched weights $(1 - s/m_\tau^2)^k$ for degrees one to four. We can see that weights of higher pinching decrease faster, which comes in handy if we want to suppress DV.

where k is the degree of the pinched weight. The higher the degree of the pinching, the lower the contribution of the critical region close to the real axis (see. fig. 1.2). Thus for higher pinchings, we are better protected from DV effects. For the transversal component of the inclusive τ decay ratio (eq. 1.1.2) a pinching of second degree appears quite naturally as the kinematic weight (see **??**). In general, it is said that a double pinched weight is sufficient to neglect effects caused by DV. In our analysis, we show that double pinched weights indeed sufficiently suppress DV and that even single pinched weights lead to acceptable results. Next, to applying pinched weights, we focus on combinations of vector and axial-vector contributions, which as we will see, regarding the ALEPH data have visibly suppressed DV.

1.4 Borel Summation

The Adler function of eq. 1.1.5 is given by a divergent asymptotic series. We only know the needed Adler function coefficients $c_{n,m}$ up to fifth order. To get

the best possible sum for such a series we can apply the *Borel summation* (BS). The BS is a long known summation method for divergent series introduced by Émile Borel [**Emile1899**].

Regarding the sum

$$A = \sum_{n=0}^{\infty} a_k \tag{1.4.1}$$

we can introduce the faculty of n, which can be rewritten in its integral form

$$A = \sum_{n=0}^{\infty} \frac{n!}{n!} a_k = \sum_{n=0}^{\infty} \frac{a_k}{n!} \int_0^{\infty} e^{-t} t^n \, dt. \tag{1.4.2}$$

Interchanging the integral and the sum is referred to as the *Borel integral*

$$A \equiv \int_0^{\infty} dt e^{-t} \sum_{n=0}^{\infty} \frac{a_k}{n!} t^n, \tag{1.4.3}$$

which contains the *Borel transform*

$$B[A](t) = \sum_{n=0}^{\infty} \frac{a_k}{n!} t^n. \tag{1.4.4}$$

The Borel integral is only valid for Borel transforms with no singularities for real positive t. In the cases of a valid Borel integral, the BS can now be used to get exact answers of divergent series, by first applying the Borel transform and then integrating over it, with the help of the Borel integral.

In our case, we want to calculate the BS of the Adler function given in eq. 1.1.5 to argue if FOPT or CIPT gives the better approximation to the τ decay ratio. For convenience, the Adler function is redefined by

$$\frac{12\pi^2}{N_c} D_V^{1+0}(s) \equiv 1 + \widehat{D}(s) \equiv 1 + \sum_{n=0}^{\infty} r_n \alpha_s(\sqrt{(s)})^{n+1}. \tag{1.4.5}$$

Following the BS prescription, we apply the Borel transformation to $\widetilde{D}$

$$B[\widehat{D}](t) \equiv \sum_{n=0}^{\infty} r_n \frac{t^n}{n!} \quad \text{with} \quad t \in C. \tag{1.4.6}$$

As t is a complex number we can study the Borel transform in the so-called *Borel plane*. The Borel plane for the Adler function is visualised in fig. 1.3. For real t the Borel transform of the Adler function has poles. Poles of the

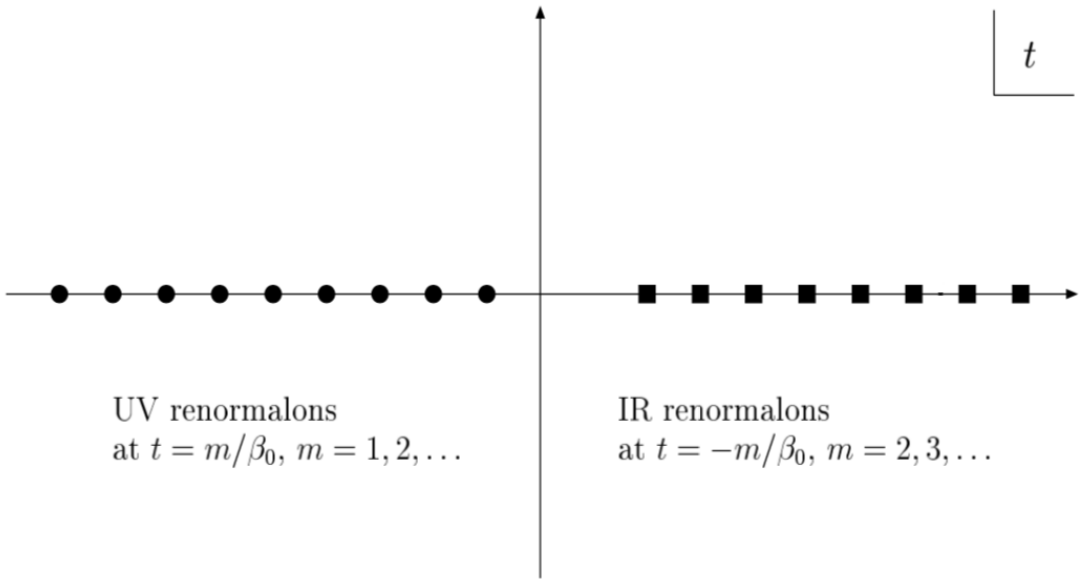

Figure 1.3: Singularities in the Borel plane of the Adler function, taken from[**Beneke1998**].

Borel transform are referred to as renormalons [**Beneke1999**, **Zichichi1979**]. We have to distinguish between *ultraviolet* (UV) and *infrared* (IR) renormalons. UV renormalons are located at $t = m/\beta_0$ with positive integer $m = 1, 2, \ldots$ and IR renormalons are located at $t = -m\beta_0$ with positive integer $m = 2, 3, \ldots$. The Borel integral of the redefined Adler function is given by

$$\widehat{D}(\alpha) \equiv \int_0^\infty dt e^{-t/\alpha} B[\widehat{D}](t). \tag{1.4.7}$$

It is not well defined, due to poles of the positive real axis. Consequently, to have a valid Borel integral we have to move the contour above or below the singularities.

The ansatz we use to express the Adler function in terms of the BS was introduced by Beneke et al. [**Beneke2008**]. They have built a physical model for the Adler function series

$$B[\widehat{D}](u) = B[\widehat{D}_1^{UV}](u) + B[\widehat{D}_2^{IR}](u) + B[\widehat{D}_3^{IR}](u) + d_0^{PO} + d_1^{PO} u, \tag{1.4.8}$$

where $B[\widehat{D}_p^{UV/IR}](u)$ are ansätze for the ultraviolet and infrared appearing renor-

malon poles

$$B[\widehat{D}_p^{IR}](u) \equiv \frac{d_p^{IR}}{(p-u)^{1+\tilde{\gamma}}}\left[1+\tilde{b}_1(p-u)+\tilde{b}_2(p-u)^2+\dots\right] \tag{1.4.9}$$

$$B[\widehat{D}_p^{UV}](u) \equiv \frac{d_p^{UV}}{(p+u)^{1+\bar{\gamma}}}\left[1+\bar{b}_1(p+u)+\bar{b}_2(p+u)^2\right], \tag{1.4.10}$$

which have been defined in section five of [**Beneke2008**]. As the large order behaviour of the Adler function is governed by a sign-alternating UV renormalon divergence and the lower-orders are not, only the leading UV singularity has been included. Furthermore, the intermediate orders are governed by IR renormalons. Thus the first two ($m = 2$ and $m = 3$) have been included into the model. The five parameters d_1^{UV}, d_2^{IR}, d_3^{IR}, d_0^{PO} and d_1^{PO} have then to be matched to the known perturbative expansion of the Adler function. They are found to be [**Beneke2008**]

$$\begin{aligned} d_1^{UV} = -0.0156, \quad d_2^{IR} = 3.16, \quad d_3^{IR} = -13.5, \\ d_0^{PO} = 0.781 \quad \text{and} \quad d_1^{PO} = 0.00766. \end{aligned} \tag{1.4.11}$$

We will apply the Borel integral of this model to perform fits as an alternative to FOPT.

1.5 Experiment

The τ decay data we use to perform our QCD analysis is from the ALEPH experiment. The ALEPH experiment was located at the *large-electron-positron* (LEP) collider at *European Organisation for Nuclear Research* (CERN) in Geneva. LEP started producing particles in 1989 and was replaced in the late 90s by the *large-hadron-collider* (LHC), which makes use of the same tunnel of 27 km circumference. The data produced within the experiment is still maintained by former ALEPH group members led by M. Davier, which have performed regular updates on the data-sets [**Davier2013**, **Davier2008**, **Aleph2005**]. The last update was motivated by Boito et al. [**Boito2010**], who discovered irregularities in the covariances by comparing data from a Monte Carlo generator with the ALEPH.

The measured spectral functions for the ALEPH data are defined in [**Davier2007**] and are given for the transverse and longitudinal components separately

$$\begin{aligned}\rho^{(1)}_{V/A}(s) &= \frac{m_\tau^2}{12|V_{ud}|^2 S_{EW}} \frac{\mathcal{B}(\tau^- \to V^-/A^- \nu_\tau)}{\mathcal{B}(\tau^- \to e^- \overline{\nu}_e \nu_\tau)} \\ &\quad \times \frac{dN_{V/A}}{N_{V/A}\, ds} \left[\left(1 - \frac{s}{m_\tau^2}\right)^2 \left(1 + \frac{2s}{m_\tau^2}\right)\right]^{-1} \\ \rho^{(0)}_{A}(s) &= \frac{m_\tau^2}{12|V_{ud}|^2 S_{EW}} \frac{\mathcal{B}(\tau^- \to \pi^-(K^-)\nu_\tau)}{\mathcal{B}(\tau^- \to e^- \overline{\nu}_e \nu_\tau)} \times \frac{dN_A}{N_A\, ds} \left(1 - \frac{s}{m_\tau^2}\right)^{-2}.\end{aligned} \tag{1.5.1}$$

The data relies on a separation into vector and axial-vector channels. In the case of the π this can be achieved via counting. The vector channel is characterised by a negative G-parity, whereas the axial-vector channel has positive G-parity. A single π carries negative G-parity, thus an even number of π carries positive G-parity and an odd number of π carry negative G-parity:

$$n \times \pi = \begin{cases} \text{vector} & \text{if } n \text{ is even,} \\ \text{axial-vector} & \text{otherwise.} \end{cases} \tag{1.5.2}$$

The separation into vector and axial-vector channel of mesons including strange quarks, like $K\overline{K}$ pairs, is more difficult because these are not in general eigenstates of G-parity and contribute to both V and A channels.

The contributions to the spectral function for the vector, axial-vector and V+A channels can be seen in fig. 1.4. The dominant modes in the vector case are decays into two ($\tau^- \to \pi^-\pi^0\nu_\tau$) or four ($\tau^- \to \pi^-\pi^-\pi^+\pi^0\nu_\tau$) pions [**Davier2006**]. The first of these is produced by an intermediate $\rho(770)$ meson, which in contrary to the pions carries angular momentum of one and is clearly visible as peak around 770 GeV in fig. 1.4a. The dominant modes in the axial-vector case are decays into one ($\tau^- \to \pi^-\nu_\tau$) or three ($\tau^- \to \pi^-\pi^0\pi^0\nu_\tau$ and $\tau^- \to \pi^-\pi^-\pi^+\nu_\tau$) pions. Here the three pion final states stem from the a_1^--meson, which can be seen as a peak in fig. 1.4b.

We furthermore added the perturbative contribution for a fixed $\alpha_s(m_\tau) = 0.329$ using FOPT in fig. 1.4c. We can see, that the perturbative contribution (the blue line) is an almost straight line and cannot reproduce the oscillating behaviour, given by the ALEPH data. This is especially the case for the not combined V

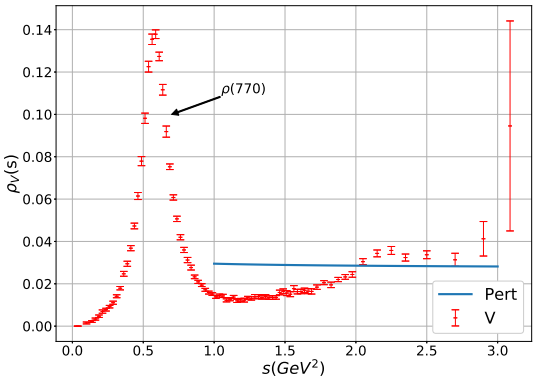

(a) Vector

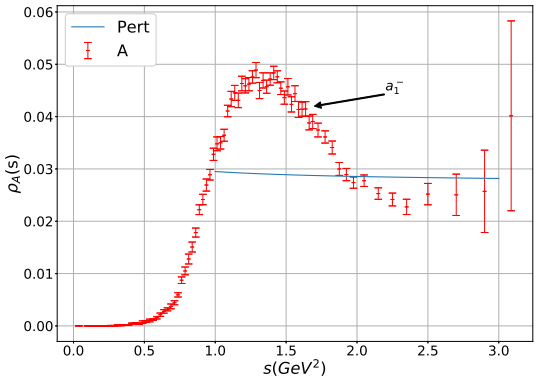

(b) Axial-Vector

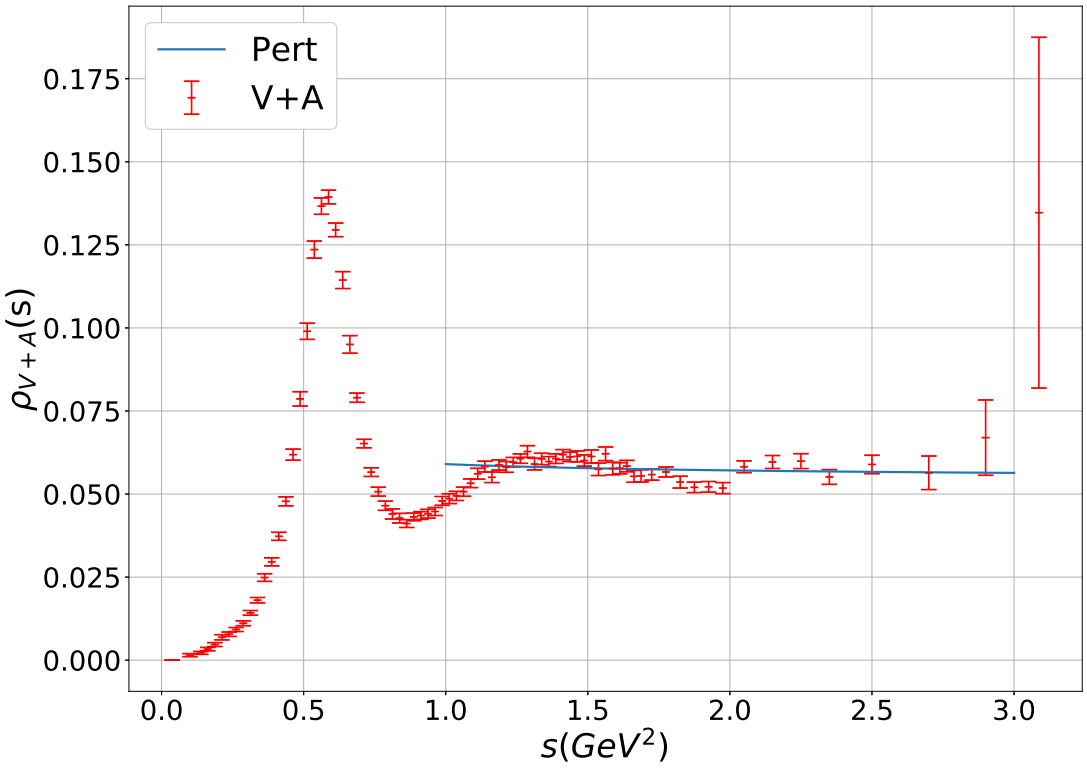

(c) Vector plus Axial-Vector

Figure 1.4: Visualisation of the vector, axial-vector and V+A spectral function given by the ALEPH data [**Davier2013**] in red with errors. We also plotted the FOPT theoretical calculation up to third order in α_s, for a fixed $\alpha_s(m_\tau^2) = 0.329$ in blue. Note that the perturbative contributions cannot fully represent the experimental data. They do not reproduce the sinusoidal form.

and A channel and is seen as an indicator for DV. Even including NP, higher dimensions of the OPE is not reproducing the wavy structure. In the case of V+A channel, we have a higher agreement between our perturbative graph and the data. In general, we believe that DV are sufficiently suppressed if we limit ourselves to data from the V+A channel. We will argue in favour of this statement in the following chapter. This is only the case for energies larger than $1.5\,GeV$, as the ρ resonance of the V channel is impossible to be represented by perturbative tools. For lower energies DV become too important to be neglected.

1.5.1 Total τ Decay Ratio from Experimental Data

The data has been last revised in 2014 [**Davier2013**] and is publicly available [**AlephData**]. It consists of the mass squared bin centre (*sbin*), the bin size (*dsbin*), the normalised invariant mass squared distribution (*sfm2*), the total errors (*derr*) and their correlations (*corerr*). To make the data comparable to our theoretical calculations we have to give the normalised invariant mass squared distribution (*sfm2*) in the form of the total decay ratio R_τ. The data is given as the normalised invariant mass squared distribution $(dN_i/ds)/N_i$ scaled by a factor 100 and further normalised to the corresponding branching ratio $i \in \{V,A,V+A\}$. Thus we can connect the branching ratio of the i^{th} channel to *sfm2* as follows

$$\mathcal{B}_{V/A} \equiv \int_0^{s_\tau} ds \frac{sfm2_{V/A}(s)}{100} \equiv \int_0^{s_\tau} ds \mathcal{B}_{V/A} \left(\frac{dN_{V/A}}{N_{V/A}\, ds} \right), \tag{1.5.3}$$

where we used $s_\tau \equiv m_\tau^2$. The total decay ratio R_τ is defined as the ratio τ decaying into hadrons and τ decaying into electrons. It and can be expressed via the corresponding branching ratios, which can be connected to the invariant mass squared distribution sfm2

$$R_{\tau,V/A} = \frac{\mathcal{B}_{V/A}}{\mathcal{B}_e} = \int_0^{s_\tau} ds \frac{sfm2_{V/A}(s)}{100\mathcal{B}_e}. \tag{1.5.4}$$

Theoretically, the decay ratio is given in eq. 1.0.1. If we neglect the longitudinal contribution $\mathrm{Im}\,\Pi^{(0)}(s)$ and remember the definition of the spectral function

(**??**) and the kinematic weight (**??**), we can write the decay ratio as

$$R_{\tau,i} = \int_0^{s_\tau} \frac{ds}{s_\tau} \omega_\tau(s) \rho(s) \tag{1.5.5}$$

and thus relate the spectral function to the experimental data

$$\rho(s) = \frac{s_\tau}{12\pi^2 100 \mathcal{B}_e} \frac{sfm2}{\omega_\tau}. \tag{1.5.6}$$

To fit the experimental data we define a so-called *spectral function moment* (or *moment*)

$$I_i^{exp,\omega} \equiv \int_0^{s_0} \frac{ds}{s_0} \omega \left(\frac{s}{s_0} \right) \rho(s), \tag{1.5.7}$$

which will be used in our χ^2 fits, explained in the upcoming section. The data is given for discrete bins so we have to express the integral of the spectral function moment as a sum over those bins. The final expression we use to fit parameters to the experimental data is then given by

$$I^{\omega}_{exp,V/A}(s_0) = \frac{s_\tau}{100 \mathcal{B}_e s_0} \sum_{i=1}^{N(s_0)} \frac{\omega\left(\frac{s_i}{s_0}\right)}{\omega_\tau\left(\frac{s_i}{s_\tau}\right)} sfm2_{V/A}(s_i). \tag{1.5.8}$$

1.6 The Method of Least Squares

We apply the *method of least squares* (LS) to fit the parameters $\vec{\alpha}$ from the experimental data. Our χ^2-function can be expressed as

$$\chi^2 = \left(I_i^{exp} - I_i^{th}(\vec{\alpha}) \right) C_{ij}^{exp\,-1} \left(I_j^{exp} - I_j^{th}(\vec{\alpha}) \right), \tag{1.6.1}$$

where I^{exp}/I^{th} is a vector of experimental moments/theoretical moments with the same weight, but different energy cutoffs s_0, labelled by the indeces i and j. C^{exp} is the covariance matrix describing the correlation of the different experimental moments $C_{ij}^{exp} = cov[I_i^{exp} I_j^{exp}]$, which can be computed by the given correlation matrix of the ALEPH data.

We aim to minimise the value of χ^2, which will fix the parameter vector $\vec{\alpha}$. The properties of the χ^2-function are well known and the best fits are characterised through $\chi^2/dof \approx 1$, where the DOF of the fit can be calculated through

$$\text{DOF} = \text{experimental moments} - \text{parameters}. \tag{1.6.2}$$

E.g. if we want to fit α_s and the dimension four Wilson coefficient C_4 we get $7-2=5$ dof.

The values we obtain for χ^2/dof for stable fits are smaller than one. We explain this behaviour with missing correlations in the aleph data. In general we will declare fits with an $\chi^2/\mathrm{dof} < 1$ as having a good χ^2 if the chi^2 is not close to zero.

For our purposes, we use the numerical minimisation computer program minuit, which was originally written in fortran by Fred James in the seventies [**James1975**]. Today in its second version the program has been ported to C++ by the root [**Brun1997**] project at cern.

The parameter vector $\vec{\alpha}$ includes the strong coupling α_s, and higher dimensional ope contributions. We should have at least as many, if not more moments as the parameters count. We are limited to fit a set of only a few parameters, because moments of similar weights are highly correlated.

It is possible to increase the number of moments used by applying multiple weights ω. Unfortunately using different weights leads to even higher correlated moments, which cause numerical complications in inverting the covariance matrix in eq. 1.6.1. To handle the high correlations we have to redefine our fit quality.

1.6.1 Block Diagonal "Fit-Quality"

For fits including multiple weights, which we do not perform in this work, we can redefine ls [**Boito2014**] to

$$Q^2 = \sum_{\omega} \sum_{s_0^i, s_0^j} \left(I_\omega^{exp}(s_0^i) - I_\omega^{th}(s_0^i, \vec{\alpha}) \right) \widetilde{C}^{-1}_{ij,\omega} \left(I_\omega^{exp}(s_0^j) - I_\omega^{th}(s_0^j, \vec{\alpha}) \right), \qquad (1.6.3)$$

where the covariance matrix $\widetilde{C}$ is now a diagonal of the experimental covari-

ance matrices C_{ω}^{exp} for each weight

$$\widetilde{C} = \begin{pmatrix} C_{\omega=1}^{exp} & 0 & \dots & 0 \\ 0 & C_{\omega=2}^{exp} & \ddots & \vdots \\ \vdots & \ddots & \ddots & 0 \\ 0 & \dots & 0 & C_{\omega=n}^{exp} \end{pmatrix}. \tag{1.6.4}$$

As a result, we are still able to invert the newly defined covariance matrix $\widetilde{C}$, but minimisation routines like CERN minuit are not able to calculate the proper errors for the parameters we want to extract. We have to perform our own error propagation to obtain meaningful errors for the parameters. The error propagation has been derived in [**Boito2011a**, **Boito2011**] and is given as

$$\langle \delta\alpha_k \alpha_l \rangle = A_{km}^{-1} A_{ln}^{-1} \frac{\partial I_i^{th}(\vec{\alpha})}{\partial \alpha_m} \frac{\partial I_r^{th}(\vec{\alpha})}{\partial \alpha_n} \widetilde{C}_{ij}^{-1} \widetilde{C}_{ij}^{-1} \langle \delta I_k^{exp} \delta I_l^{exp} \rangle, \tag{1.6.5}$$

where

$$A_{kl} = \frac{\partial I^{th}(\vec{\alpha})}{\partial \alpha_k} C_{ij}^{-1} \frac{I_j^{th}(\vec{\alpha})}{\alpha_l}. \tag{1.6.6}$$